

Numerical study of stochastic particle dispersion using One-Dimensional-Turbulence

Marco Fistler*¹, David O. Lignell ², Alan Kerstein³ and Michael Oevermann¹

¹Department of Applied Mechanics, Chalmers University of Technology, Sweden

²Brigham Young University, Provo, UT 84602, USA

³Consultant, 72 Lomitas Road, Danville, CA 94526, USA

Abstract

A stochastic model to study particle dispersion in a round jet configuration using the one-dimensional-turbulence model (ODT) is evaluated. To address one of the major problems for multiphase flow simulations, namely computational costs, the dimension-reduced model is used with the goal of predicting these flows more efficiently. ODT is a stochastic model simulating turbulent flow evolution along a notional one-dimensional line of sight by applying instantaneous maps which represent the effect of individual turbulent eddies on property fields. As the impact of the particles on the carrier fluid phase is negligible for cases considered, a one-way coupling approach is used, which means that the carrier-phase is affecting the particle dynamics but not vice versa. The radial dispersion and axial velocity are compared with jet experimental data as a function of axial position. For consistent representation of the spatially developing round jet, the spatial formulation of ODT in cylindrical coordinates is used. The investigated jet configuration has a nozzle diameter of 7 mm and Reynolds numbers ranging from 10000 to 30000. The flow statistics of the ODT particle model are compared with experimental measurements for two different particle diameters (60 and 90 μm), thereby testing the Stokes number dependence predicted by ODT.

*Corresponding Author: marco.fistler@chalmers.se

Introduction

For a wide spectrum of disciplines turbulent dispersed two-phase flows are of particular interest with respect to understanding the physical fundamentals of these flows. Dispersed two-phase flows are very difficult to investigate experimentally and only a few advanced techniques to obtain spatially resolved unsteady data exist today. CFD (computational fluid dynamics) is a very powerful tool with which to investigate turbulent dispersed flows and acquire detailed flow information. However, many CFD approaches for turbulent dispersed flows rely on many modeling assumptions and their predictive capabilities are limited. Due to the extremely high costs of direct numerical simulation (DNS) studies of particle-laden flows, their application so far is limited to academic cases and systems with relatively low particle numbers. Large eddy simulations (LES) incorporating a model to capture the sub-grid-scale turbulence predict well the unsteadiness of turbulence, but the accuracy of the results is very dependent on several LES parameters and the chosen subgrid-model.

In this study an alternative approach called one-dimensional turbulence (ODT) is used. ODT is a stochastic approach with reduced dimensionality to resolve affordably the full range of length and time scales as in a DNS. While molecular phenomena like viscous dissipation evolve along that single dimension, the turbulent cascade is modeled through stochastically sampled remappings of the velocity profiles, called eddy events. Schmidt et al. [1, 2] and Sun et al. [3] extended the ODT model to predict particle laden flow in different configurations. These formulations assume an instantaneous in time (referred to as Type-I) particle-eddy interaction and showed promising results in homogeneous turbulence and turbulent channel flow. One limitation was the need to compare the temporal ODT output data with spatial experimental results. Here the work of [1, 2] and [3] is continued and extended by using a spatial formulation of ODT in cylindrical coordinates. The present study is based on the same test case as in [3].

One-dimensional turbulence

One-dimensional turbulence was developed by Kerstein [4] as a stochastic model that generates unsteady solutions of turbulent flows on a one-dimensional domain. This domain is usually oriented in the direction of the largest expected velocity gradients, e.g. in the lateral/radial direction for simulating a turbulent dispersed jet configura-

tion. In a Lagrangian setting its basic elements are the momentum balance for the three momentum components omitting advection and pressure forcing and a stochastic model for turbulent advection. This model is based on so-called eddy events in which the velocity profiles are remapped. In the present spatially advanced cylindrical formulation, first mentioned in [5], the radially (r) oriented ODT line plus the direction (z) of spatial advancement can be interpreted in each realization as an instantaneous snapshot of a 2D cut through the 3D flow field. The underlying flow in the Lagrangian frame of reference is governed by the steady solution of the momentum equation derived from the Reynolds theorem. The unsteadiness is captured by a random sequence of eddy events and so the model obeys the conservation laws of statistically steady flows but also reflects unsteadiness due to turbulence. Namely, due to different spatial development in each realization, a set of simulated realizations is the ODT analog of a statistical ensemble of turbulent flow states. This formulation for ODT was introduced in [4] and discussed in more detail in [6].

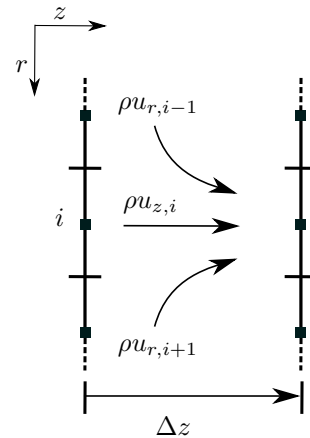


Figure 1: Illustrative sketch of mass flux balance between spatial steps

GOVERNING EQUATIONS

ODT evolution equations are obtained by considering the balances of mass and momentum flux crossing cell boundaries within the axial interval z_0 to $z_0 + \Delta z$; see Fig. 1. The balance equation for the mass flux is

$$\frac{1}{r} \frac{\partial(r\rho u_r)}{\partial r} + \frac{\partial(\rho u_z)}{\partial z} = d_{\rho u_z}, \quad (1)$$

where the cell velocities in the evolving and the line direction are u_z and u_r , respectively. $d_{\rho u_z}$

represents the changes during eddy events happening between z_0 and $z_0 + \Delta z$ due to mapping and re-distributions of energy components. This value is zero if there are no eddy event events within the Δz interval, otherwise its value is determined by the mapping process described below.

The control-volume balance equation for each component of momentum flux is

$$\frac{\partial(r\rho u_i u_z)}{\partial z} + \frac{\partial(r\rho u_i u_r)}{\partial r} = \frac{\partial}{\partial r} \left(r\mu \frac{\partial u_i}{\partial r} \right) + d_{\rho i u_z}, \quad (2)$$

where μ is the dynamic viscosity and $d_{\rho i u_z}$ represents, as in the mass flux balance, the sudden changes during eddy events happening between z_0 and $z_0 + \Delta z$, which are balanced as gains or losses at the cell boundaries. Outside the eddy region they are zero. For this study the density ρ is constant and the pressure gradient is zero, so the pressure term is omitted.

EDDY EVENTS

As mentioned above, turbulent advection is modeled through eddy events re-mapping the velocity and all other property profiles over a sampled eddy region $r_0 < r < r_0 + l$ characterized by a position r_0 and a length scale l . Eddy location and size are randomly sampled to mimic turbulent eddy occurrences in reality. Triplet mapping is used as the mapping method in ODT, which means in a planar coordinate system that each profile is compressed by a factor of three and three copies of it fill the sampled region. The second copy in the middle is inverted to conserve the continuity of the profile (illustrated in [4]). Instead of considering the eddy region as just the length of the eddy, in a cylindrical system the region is represented as the area above (seen in Fig. 2). The triplet map function $f(r)$, which describes the pre-triplet map fluid position as function of the post-position, is given for the case $r_0 \geq 0$ as

$$f(r) = r_0 + \begin{cases} \sqrt{3(r-r_0)^2} & \text{if } r_0 \leq r \leq r_0 + \sqrt{\frac{l^2}{3}} \\ \sqrt{2l^2 - 3(r-r_0)^2} & \text{if } \sqrt{\frac{l^2}{3}} \leq r \leq \sqrt{\frac{2l^2}{3}} \\ \sqrt{3(r-r_0)^2 - 2l^2} & \text{if } \sqrt{\frac{2l^2}{3}} \leq r \leq l \\ r - r_0 & \text{otherwise.} \end{cases} \quad (3)$$

For the case $r_0 < 0$ the algebraic signs have to be adjusted in consideration of the possibilities $r_0 + l$ is greater or smaller zero. For re-distributing energy among the velocity components kernel transformations are introduced, which add or subtract energy from velocity profiles. The reason for the re-distribution is the return-to-isotropy phenomenon of turbulent flows going from larger to smaller scales.

As a result, the eddy region is mapped as

$$u_i(r) \rightarrow u_i(f(r)) + c_i K(r). \quad (4)$$

The kernel $K(r)$ is defined as the fluid displacement profile under a triplet map and obeys $\int_{r_0}^{r_0+l} K(r)r dr = 0$. c_i is the kernel coefficient and defines the kernel amplitude. Due to its measure preserving property all integral properties and moments remain constant during a triplet map. Of particular interest is the conserved kinetic energy. It is used to determine the eddy timescale $\tau_e(l, r_0)$, which is the last eddy parameter after position and length to define an eddy event. Scaling arguments are used to relate a measure E_{kin} of the available kinetic energy within the sampled eddy to the eddy timescale, $E_{kin} \sim \frac{\rho l^3}{2\tau_e^2}$. This motivates

$$\frac{1}{\tau_e} = C \sqrt{\frac{2}{\rho l^3} (E_{kin} - Z E_{vp})}. \quad (5)$$

The viscous penalty energy is given as $E_{vp} = \frac{\mu^2}{2\rho l}$. C is the adjustable eddy rate parameter and scales the overall eddy event frequency. Z is the viscous penalty parameter, which controls the suppression of unphysically small eddies. The same is done for large eddies using the elapsed time method, in which the eddy time can be compared with the simulation elapsed time t . Eddy events are only allowed when $t \geq \beta\tau_e$, where β is another model parameter.

We assume that the occurrence of eddies with given r_0 and l follows a Poisson process in time with a rate determined by the eddy timescale provided in (5). Technically this is implemented by oversampling, i.e. generation of candidate eddies at a much higher rate than needed, and thinning of the Poisson process with an acceptance-rejection method. For details we refer to [7].

Lagrangian particle model

Due to the very small ratio of particle mass to fluid mass in cases considered here, a one-way coupling between particle and gas phase is assumed, which means the particle phase has no influence on the fluid phase. Similar to the ODT structure, the particle model is separated into two parts. The first one is the particle advancement due to the underlying flow field and the second is governed by so-called particle-eddy interactions (PEI).

The gas velocity of the underlying flow field affects particle motion according to the particle drag

law, which is given as

$$\begin{aligned} \frac{du_{p,i}}{dt} &= -\frac{u_{p,i} - u_{g,i}}{\tau_p} f + g_i, \\ \frac{dr_p}{dt} &= u_{p,r}. \end{aligned} \quad (6)$$

Here, the subscript p and g represent the particle and gas phase, respectively. g_i is the i -th component of the gravity acceleration vector. The particle response time, $\tau_p = \frac{\rho_p d_p^2}{18\mu}$ based on Stokes flow, is given in terms of the diameter d_p and density ρ_p of the particle and the fluid viscosity μ . Clift et al.[8] suggested a non-linear correction factor f for a particle slip-velocity Reynolds number, $Re = \frac{\rho_g |\vec{u}_p - \vec{u}_g| d_p}{\mu}$, smaller than 200, which holds for the present cases as well as many practical dilute flow systems. The factor f is defined as

$$f = 1 + 0.15 Re_p^{0.687}. \quad (7)$$

For the PEI model used here and described in the following section, the PEI is the only effect of the gas phase on the particle phase for the ODT line-directed motion and so it is defined that the gas velocity in this direction for the drag law (6) is zero. The drag law (Eq. 6) is solved by a first-order Euler method. As the ODT line evolves in spatial coordinate (Δz), the temporal step Δt should be transformed. Therefore, a constant particle velocity over Δz is assumed, which yields

$$\Delta t = \frac{\Delta z}{u_{p,z}}. \quad (8)$$

PARTICLE-EDDY INTERACTION MODEL

Schmidt et al. [1, 2] developed multiple PEI models for different applications. In this study the instantaneous (type-I) PEI model is implemented. The model is applied to a particle if it is located in the sampled eddy region. For solution of the particle's equations of motion (6) during an eddy event we need to define an eddy gas phase velocity $u_{g,i}$ and a particle interaction time τ_{PEI} which defines the time interval for the integration in time of (6).

In the instantaneous PEI model the gas phase velocity $u_{g,r}$ is determined using the concept of a mass-less tracer particle following the flow instantaneously, i.e. the location of a tracer particle after the particle-eddy interaction is determined by the triplet-map (3) only. As illustrated in Fig. 2, the triplet map provides three different post-map particle locations, so a unique position is sampled

randomly from those three positions. The resulting particle displacement ΔR_{TM} is then used with the eddy time τ_e in (5) to define the gas phase velocity in direction of the ODT line as $u_{g,r} = \Delta R_{TM}/\tau_e$. The other two velocity components are taken from the gas phase velocity at the original location of the particle. The particle interaction time τ_{PEI} is defined as the earliest time when the particle leaves the eddy space-time box [$l \times l \times \beta_p \tau_e$]. β_p is a model parameter, which defines the interaction time length of particle and eddy. To find the interaction time, Stokes law is modified and analytically solved to find the earliest time when the particle leaves the space-time eddy box. The initial position of the particle in the lateral direction is assumed to be the lateral mid-point.

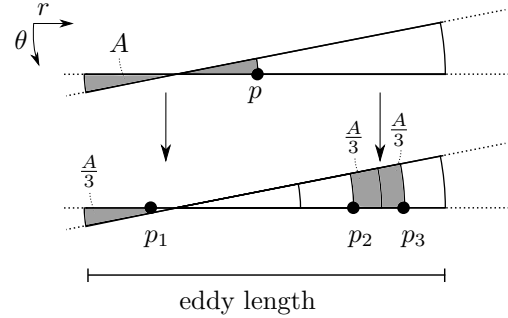


Figure 2: Illustration of particle displacement by a cylindrical triplet map

Test case

EXPERIMENTS

The aim of this study is to validate the numerical model extension with the measurements of Kennedy and Moody [9]. They studied turbulent dispersion of particles in shear-dominated flows and span a range of Reynolds and Stokes numbers by varying the jet velocity, nozzle diameter and particle diameter. In this work we vary the jet velocity for Reynolds number of 10000, 20000 and 30000 and investigate the particle diameters 60 and 90 μm . The hexadecane droplets have a density of $\rho_p = 770 \frac{\text{kg}}{\text{m}^3}$ and have a tolerance of their diameter of 2 μm . The experiments were performed at standard room temperature and pressure, thus the particles are non-vaporizing. In the streamwise direction a nonzero gravity effect must be considered. Table 1 shows the initial conditions of the particle and gas phases for each test case. The initial jet velocities are based on the Reynolds numbers with a jet exit diameter of 7 mm.

	Re=10 ⁵	Re=2 · 10 ⁵	Re=3 · 10 ⁵
$u_{g,z0}$	21.5 m/s	43 m/s	64.5 m/s
$u_{p,z0}(60\mu\text{m})$	17.5 m/s	30 m/s	46 m/s
$St(60\mu\text{m})$	26	53	77
$u_{p,z0}(90\mu\text{m})$	15 m/s	32 m/s	51.5 m/s
$St(90\mu\text{m})$	61	122	178

Table 1: Initial conditions of the particle and gas phases

SIMULATION SETUP

As the initial jet profile on the ODT domain the following function is used

$$u_{g,z}(r) = \frac{u_{g,z0}}{2} \left[\left(1 + \tanh\left(\frac{r - L_1}{\omega_l}\right) \right) \times \left(1 - \frac{1}{2} \left(1 + \tanh\left(\frac{r - L_2}{\omega_l}\right) \right) \right) \right]. \quad (9)$$

L_1 and L_2 are the middle positions of the transitions and ω_l is the transition boundary layer width.

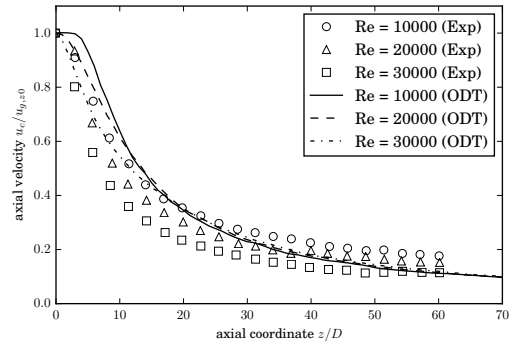
This study uses 512 ODT realizations, which Sun et al.[3] reported as sufficient to capture stationary statistics.

Results

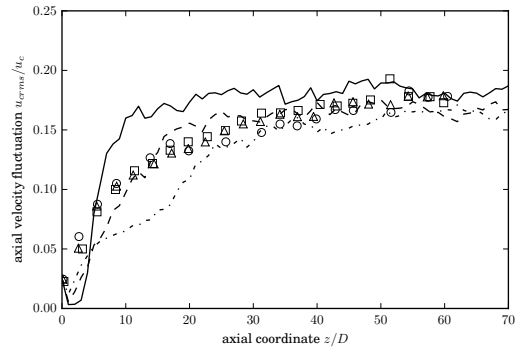
GAS PHASE

For the assessment of the gas-solid particle interaction, the first step is to achieve reasonable agreement of the gaseous flow between experiments and ODT simulations. A viscous penalty parameter $Z = 400$ with an eddy frequency parameter $C = 12$ resulted in overall agreement which is shown in Fig. 3a and 3b for axial mean velocity and the turbulence intensity along the centerline.

The axial positions z , mean axial velocities $u_{c,z}$ and turbulent intensities are normalized by the jet exit diameter D , the jet exit velocity $u_{g,z0}$ and the axial mean velocity $u_{c,z}$, respectively. The graphs of the axial mean velocities at the centerline show a similar behavior as the experimental data for different Reynolds numbers. However, they are slightly overpredicted near the jet exit, where the experimental jet velocity gradients are greater. The reason could be an under-predicted turbulent intensity at this point, which would enforce diffusion and accelerates the velocity decay. Fig. 3b shows more significant differences for the turbulent intensities for the ODT simulations with respect to the Reynolds numbers than the experiments.



(a) Mean axial velocity on centerline



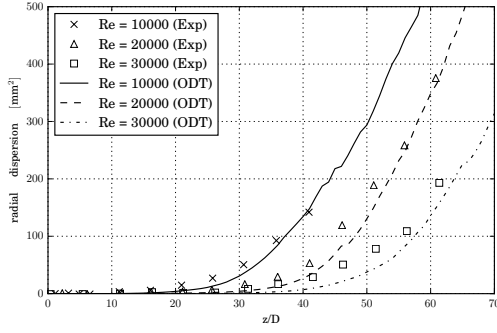
(b) Mean turbulent intensity on centerline

Figure 3: Properties of jet configuration compared with experimental data

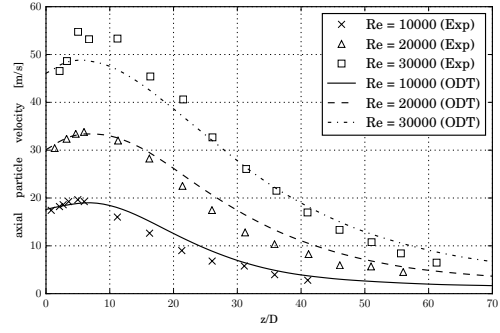
PARTICLE PHASE

In this study a particle-eddy interaction parameter $\beta_p = 0.008$ is used for the entire simulation time based on a previous parameter study, which is not discussed in this work. Presented in Figs. 4 and 5 are the results for the dispersion (a) and axial velocities (b) of the particles, respectively. The position in the streamwise direction is normalized by the jet exit diameter D .

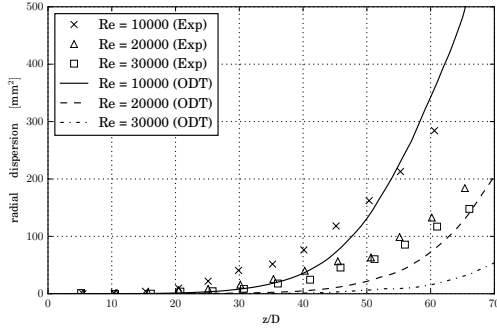
As seen in Fig. 4a, the results of a particle with a diameter of 60 μm agree very well with the experimental data. Both show that the particle dispersion is increasing with decreasing Reynolds number. For a particle diameter of 90 μm the results agree well for $Re = 10000$ and 20000, but the deviations between simulation and experimental results increases with increasing Stokes number. Both experiments and simulations show a decreasing dispersion with an increasing diameter at fixed Reynolds number corresponding to an increasing Stokes number. This



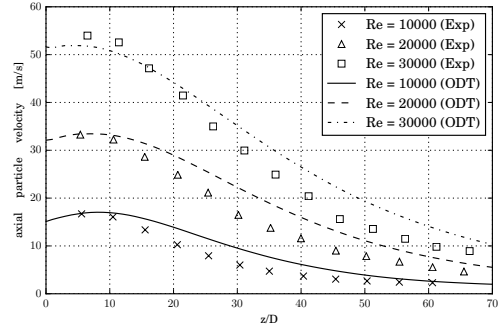
(a) $d_p = 60 \mu\text{m}$



(a) $d_p = 60 \mu\text{m}$



(b) $d_p = 90 \mu\text{m}$



(b) $d_p = 90 \mu\text{m}$

Figure 4: Mean radial dispersion of particles

Figure 5: Mean axial velocity of particles

behavior is expected due to the increasing particle response time.

The results for particle axial velocity in Fig. 5 show a continuous decay over their trajectory with a small peak at the beginning, where the particle accelerates to the fluid phase velocity. The small derivations of the velocities between experiments and simulations seem to be similar to the ones in the fluid phase and are very likely a result of them. However, the results for the axial velocity decay show that the model is capable to capture the experimental behavior of the particle phase reasonably well, both qualitatively and quantitatively.

Conclusion

The aim of this study was to develop an extension of an existing ODT model for dispersed gas-solid flow [3] by introducing spatial advancement in cylindrical coordinates for turbulent jet configurations. Modifications were made in the deterministic advancement of the particle phase and the particle-eddy interaction model. The

formulation in cylindrical coordinates required a modification of the triplet map and the particle displacement during a particle eddy interaction. The presented results show good agreement with the experimental data, reproducing the results of Sun et al. [3] without needing to transform the temporal coordinate. This is the first step of extending the ODT model for dispersed gas-solid flow using a spatial formulation. In a second step we will perform a two-way coupling between solid particles and gas phase. The future focus is to get a better understanding of the underlying physics of particle/droplet-turbulence interaction, e.g. turbulence modulation by the dispersed phase. Here, ODT can contribute by simulating cases in parameter ranges which are not accessible using conventional simulation methods such as DNS or high resolution LES.

Nomenclature

m	mass
r	radial coordinate
u_i	i-th velocity component
z	axial coordinate
ρ	density

Subscripts

0	initial
e	eddy
g	gas-phase
p	particle-phase
PEI	particle-eddy interaction
TM	triplet map

References

- [1] J. R. Schmidt, J. O. L. Wendt, and A. R. Kerstein. *IUTAM Symposium on Computational Approaches to Disperse Multiphase Flow*, Rouen, France, 2004.
- [2] J. R. Schmidt, J. O. L. Wendt, and A. R. Kerstein. *Journal of Statistical Physics*, 37:233–257, 2009.
- [3] G. Sun, D. O. Lignell, and J. C. Hewson. *International Journal of Multiphase Flow*, 89:108–122, 2016.
- [4] A. R. Kerstein. *Journal of Fluid Mechanics*, 392:277–334, 1999.
- [5] N. Krishnamoorthy. *Reaction Models and Reaction State Parameterization for Turbulent Non-premixed Combustion*, p. 75. University of Utah, Provo, Utah, 2008.
- [6] W. T. Ashurst and A. R. Kerstein. *Physics of Fluid*, 17-025107:1–26, 2005.
- [7] D.O. Lignell, A.R. Kerstein, G. Sun, and E.I. Monson. *Theoretical and Computational Fluid Dynamics*, 27(3-4):273–295, 2013.
- [8] R. Clift, J. R. Grace, and M. E. Weber. *Bubbles, drops and particle*. Academic Press, New York, 1978.
- [9] I. M. Kennedy and M. H. Moody. *Experimental Thermal and Fluid Science*, 18:11–26, 1998.